Bioorg. Med. Chem. 58 (2022) 116652

Contents lists available at ScienceDirect

Bioorganic & Medicinal Chemistry

journal homepage: www.elsevier.com/locate/bmc

Novel ferrocenylbisphosphonate hybrid compounds: Synthesis, characterization and potent activity against cancer cell lines

Chioma G. Anusionwu [a], Blessing A. Aderibigbe [b], Samson A. Adeyemi [c], Philemon Ubanako [c], Samson O. Oselusi [d], Yahya E. Choonara [c], Xavier Yangkou Mbianda [a,*]

[a] Department of Chemical Sciences, University of Johannesburg, Doornfontein Campus, Johannesburg, South Africa
[b] Department of Chemistry, University of Fort Hare, Alice Campus, Eastern Cape, South Africa
[c] Wits Advanced Drug Delivery Platform Research Unit, Department of Pharmacy and Pharmacology, School of Therapeutic Science, Faculty of Health Sciences, University of the Witwatersrand, Johannesburg, South Africa
[d] School of Pharmacy, University of the Western Cape, Bellville, Cape Town 7535, South Africa

ARTICLE INFO

Keywords:
Ferrocenylbisphosphonate hybrids
Anticancer activity
Cytotoxicity
Molecular docking

ABSTRACT

The toxicity of existing anticancer agents on healthy cells and the emergence of multidrug-resistance cancer cells have led to the search for less toxic anticancer agents with different mechanisms of action. In this study, a novel class of ferrocenylbisphosphonate hybrid compounds (**H1-H8)** were designed and characterized using NMR, IR and HRMS. The *in vitro* anticancer activity of the hybrid compounds on HeLa (cervix adenocarcinoma) and A549 (non-small cell lung cancer cell lines) was evaluated. The structure–activity relationship of the hybrid molecules was also studied. The lead compound, tetraethyl (3-(4-oxo-4-ferrocenylbutanamido) propane-1-1-diylbis (phosphonate) (**H6**) exhibited higher cytotoxicity on A549 (IC_{50} = 28.15 μM) than cisplatin (IC_{50} = 58.28 μM), while its activity on HeLa cells (IC_{50} = 14.69 μM) was equivalent to that of cisplatin 15.10 μM (HeLa cells). **H6** (IC_{50} = 95.58 μM) was also five times less toxic than cisplatin (IC_{50} = 20.86 μM) on fibroblast NIH3T3 suggesting that **H6** can be a future replacement for cisplatin due to its non-toxicity to healthy cells. Interestingly, some ferrocene and bisphosphonate parent compounds exhibited promising anticancer activity with 4-ferrocenyl-4-oxobutanoic acid (**FI)** exhibiting higher cytotoxic activity (IC_{50} = 1.73 μM) than paclitaxel (IC_{50} = 3.5 μM) on A549 cell lines. **F1** also exhibited lower cytotoxicity than paclitaxel and cisplatin on the normal murine fibroblast cell line (NIH3T3). The molecular docking studies showed **H6** strong binding affinity for the STAT3 signaling pathway in A549 cell line, and the MAdCAM-1 and cellular tumor antigen p53 proteins in HeLa cell lines.

1. Introduction

Hybrid drug design is a form of polypharmacology developed by scientists to tackle complex multifactorial diseases since the "one target, one molecule" approach could not address complex diseases. Hybrid drugs have further offered other advantages, such as low toxicity and low resistance. The application of hybrid drug strategy in the development of drugs used in the treatment of cancer,[1] malaria,[2] Alzheimer's disease,[3] HIV/AIDS,[4] tuberculosis,[5] bacterial[6] and fungal diseases[7] have been reported.

Estramustine, a hybrid of estradiol and nornitrogen mustard is clinically in use for the treatment of cancer and is probably the first hybrid drug used clinically to treat cancer.[8] Several other hybrid compounds have also been reported to exhibit anticancer activity at a nanomolar (nM) range.[9] Noh et al. developed [4-(1,3,2-dioxaborinan-2-yl) benzyl ((5-methyl-2-styryl-1,3-dioxan-5-yl) methyl) carbonate], a hybrid of quinone methide and cinnamaldehyde, which synergistically amplify oxidative stress.[10] In another report by Li et al., a series of norfloxacin/ciprofloxacin-guanidine hybrids exhibited IC_{50} of 32–116 nM against A549, HL-60 and HeLa human cancer cell lines. Their activities were better than that of their parent compounds, norfloxacin and ciprofloxacin with $IC_{50} > 302$ nM.[11] Other hybrid compounds such as napthyridinone-pyridine,[12,13] tetrazole-benzothiazole,[14] coumarin-pyrazoline[15] and coumarin-furoxan[16–18] have also been reported to exhibit high cytotoxicity on cancer cell lines.

Furthermore, for over five decades, inorganic drug molecules,

* Corresponding author.
E-mail address: mbianday@uj.ac.za (X. Yangkou Mbianda).

https://doi.org/10.1016/j.bmc.2022.116652
Received 3 October 2021; Received in revised form 29 December 2021; Accepted 28 January 2022
Available online 2 February 2022

notably, platinum-based drugs such as *cis*-dichloro-diammine-platinum (II) (cisplatin) and *cis*-diamino-(1,1-cyclobutandicarboxylate) platinum (II) (carboplatin), have been widely used in the treatment of various types of cancer, including non-small cell lung cancer and ovarian cancer. Gagnon et al.[19] reported the synthesis of a series of 17β-estradiol-linked platinum (II) hybrid molecules. These hybrid molecules presented higher affinity than 17 β-estradiol for estrogen receptor alpha (ERα) when evaluated *in vitro* on estrogen-dependent and -independent (ER^+ and ER^-) human uterine and ovarian cancer cells. Smyre et al. reported a platinum-acridine anticancer agent, which exhibited significant cytotoxicity of 40–200 folds compared to cisplatin on NCI-H460, NCI-H522 and NCI-HI435.[20] In another report, testosterone (4-androstene-17β-ol-3-one) tethered to Pt (II) moiety using 1,2,3 triazole as a linker exhibited good and highly selective activity with IC_{50} of 2.2–13.3 μM on prostate cancer lines.[21] Likewise, adenine-platinum II hybrids exhibited cytotoxicity of 1.3–4.1 μM on A549, DLD-1 and SW1736[22] while estradiol-chlorambucil hybrid was reported to exhibit higher cytotoxic activity than cisplatin on breast cancer cell lines.[23]

In addition, the success of ferroquine in clinical trials as a potential antimalarial agent has stirred more research interests in the use of ferrocene moiety for the design of drug molecules. The role of ferrocene moiety in the design of chemotherapeutic candidates has been attributed to their electrochemical activation, where oxidation to generate ferrocenium (Fc^+) species can promote the formation of reactive oxygen species (ROS).[24] Hybrids of ferrocene and tamoxifen, known as ferrocifens, are the first molecules shown to be active against both hormone-dependent and hormone-independent breast cancer cell lines[25] (Fig. 1). Ferrocene hybridized with paclitaxel[26], quinones,[27] naphthalimidines,[28] pyridines,[29] steroids,[30] aminoquinolines,[31] pyrimidines,[32] indoles,[33] flavonoids,[34] chalcones,[35] triazoles,[36] pyrazoles,[37] and benzoimidazoles[38] have shown good to excellent anticancer activity.

On the other hand, many *in vitro* pre-clinical studies have shown that the nitrogen bisphosphonates *N*-BPs are more potent than non-nitrogen bisphosphonates (non-*N*-BPs) in inhibiting cancer cell adhesion and invasion. The anticancer activity of bisphosphonates such as alendronate and pamidronate has been demonstrated *in vitro* and *in vivo* on several cancer cell lines.[39] BPs exhibit anticancer activity by inhibiting the activity of farnesyl diphosphate (FPP) synthase, a key enzyme in the mevalonate pathway. Hybridization of bisphosphonates with cisplatin enhanced their cytotoxicity against osteosarcoma MG-63 cell line,[40] while bisphosphonates conjugates such as bisphosphonate-proteasome inhibitors,[41] bisphosphonate-benzoxazole, and bisphosphonate-arylamine hybrids exhibited moderate cytotoxicity against cancer cell lines.[42] MB-11, a hybrid of cytarabine and etidronate also inhibited the proliferation of cancer cells and increased the overall survival of mice injected with myeloma cells and decreased bone tumour.[43]

Amide bond formation is one of the most critical reactions in medicinal chemistry[44] because of the neutrality, stability and hydrogen-bond accepting and donating properties of the carboxamide bond.[45] In addition, Drugs bearing amine functional groups represent an important class of therapeutic agents.[46]

Although the synthesis and kinetic drug release of macromolecular co-conjugates of bisphosphonates and ferrocene have been reported by our research group,[47] reports on the biological activities of ferrocene-bisphosphonates hybrids are extremely rare. Therefore, in our present work, a series of novel ferrocene-bisphosphonate hybrid compounds were prepared via amidation and amination. We compared the *in vitro* cytotoxicity of the hybrid compound with their parent compounds to assess the role of hybridization on the biological activities of the compounds.

2. Results and discussion

2.1. Synthesis and structures

2.1.1. Synthesis of ferrocenyl derivatives (F1, F2 and F5)

4-ferrocenyl-4-oxo-butanoic acid (**F1**) and 4-ferrocenylbutanoic acid (**F2**) were synthesized by a process described by Mukaya et al.[58]; **F1** was synthesized and obtained in 85% yield by Friedel craft acylation of

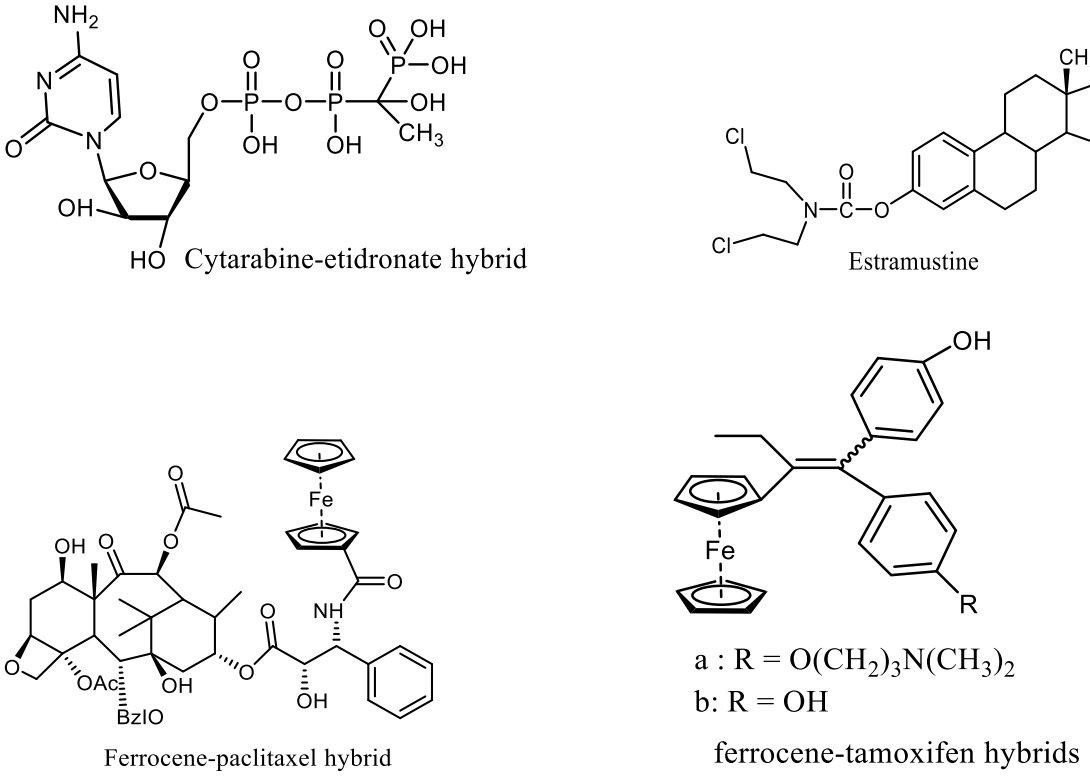

Fig. 1. Examples of hybrid chemotherapeutic agents.

ferrocene using succinic anhydride in the presence of aluminium chloride while **F2** was obtained by the reduction of **F1** through Clemmensen reduction (using Zn/Hg). In addition, ferrocenylmethyleneamine (**F5)** was synthesized by a process described by Yunsong Cai.[48] Here, ferrocenecarboxaldehye (**F4)** was reduced to ferrocene-oxime in the presence of hydroxylamine hydrochloride. The ferrocene-oxime was further reduced to ferrocenylmethyleneamine in the presence of $LiAlH_4$ to yield **F5.**

*2.1.2. Synthesis of bisphosphonates derivatives (**B1 to B4**).*

The aminobisphosphonic acids, Alendronate ((4-amino-1-hydroxy-1-phosphobutyl) phosphonate) (**B1**), ((5-amino-1-hydroxy-1-phosphopentyl) phosphonate) (**B2**) and neridronate ((6-amino-1-hydroxy-1-phosphohexyl) phosphonate) (**B3**) were synthesized from aminocarboxylic acid analogs according to a method reported by Kieczykowski et al.,[49] by reacting 4-aminobutyric acid, 5-aminovaleric acid and 6-aminocarproic acids with phosphorus trichloride (PCl_3) and phosphorus acid (H_3PO_3) in methane sulfonic acid (CH_3SO_3H) to yield **B1**, **B2** and **B3** respectively. Furthermore, tetraethylvinylidenephosphonate (**B4)** was synthesized by a two-stage process as reported in the literature;[50–52] i) reaction of tetraethylmethylene bisphosphonate (**TEMB**) with paraformaldehyde in a Horner- Wittig type reaction in the presence of diethylamine to form tetraethyl-2-methoxyethylidenebisphosphonate (**TE2MEB**), ii) reduction of **TE2MEB** to tetraethylvinylidene phosphonate (**B4)** by refluxing in toluene in a Dean-Stark apparatus. In addition, **B5** was obtained by the nitration of **B4** with nitromethane using Henry reaction and subsequent hydrogenation using Pd/c catalyst.

*2.1.3. Synthesis of ferrocene-bisphosphonate hybrid compounds (**H1-H8**)*

The synthesis of the ferrocene-bisphosphonate hybrid compounds (**H1-H8)** reported for the first time in this work occurred as follows (Fig. 2):

*2.1.3.1. Synthesis of ferrocenylaminobisphosphonic acids (**H1-H3**).* Hybrids **H1**, **H2** and **H3** were synthesized by the reductive amination of ferrocene carboxaldehyde (**F4)** with aminobisphosphonic acids (**B1**, **B2** and **B3)** using sodium cyanoborohydride as a reducing agent in a one-pot synthesis as shown in scheme 1. The two significant challenges encountered in the synthesis of this set of compounds were i) the insolubility of one of the reactants, aminobisphosphonic acid, in organic solvents and ii) difficulty in the isolation of the target compound, which is highly polar. Therefore, a method that addressed these fundamental issues was explored. A procedure described by Jiu-rong et al.,[53] for the synthesizing ferrocenylmethylene glycine was applied with little modification. In this instance, the aminobisphosphonic acids were first converted to their corresponding sodium salts by stirring the aminobisphosphonic acid with an equimolar NaOH in methanol until dissolution. The addition of NaOH aided the dissolution of the bisphosphonic acid in methanol and raised the pH of the reaction mixture from about 3 to 8. Then, ferrocenecarboxaldehyde (**F4)** in dry methanol was added, followed immediately by sodium cyanoborohydride, $NaBH_3CN$ (also in dry methanol), and the reaction mixture was stirred at room temp for 48 h. The target product was precipitated by adjusting the pH of the reaction mixture to 2–3 with 20% HCl solution. After filtration, the precipitate was washed with cold water and 95 % ethanol. Using $NaBH_4$ in place of $NaBH_3CN$ in this reaction also afforded the product, but, in this case, on addition of **F4**, the reaction mixture was stirred for about 12 h to allow for the conversion of the aldehyde to imine before the $NaBH_4$ was introduced for complete reduction.

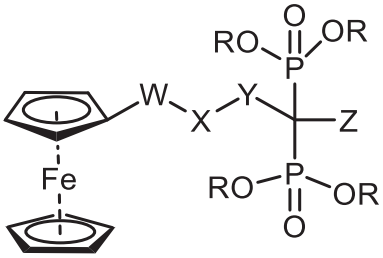

H1: W = CH_2, X = NH, Y = $(CH_2)_3$, Z = OH, R = H;
H2: W = CH_2, X = NH, Y = $(CH_2)_4$, Z = OH, R = H;
H3: W = CH_2, X = NH, Y = $(CH_2)_5$, Z = OH, R = H
H4: W = C=O, X = NH,Y = CH_2, Z = H, R = Et;
H5: W = C=O$(CH_2)_2$, X = CONH,Y = $(CH_2)_2$, Z = H, R = Et;
H6: W = $(CH_2)_3$, X= CONH,Y = ($CH_2)_2$, Z = H, R = Et;
H7: W = CH_2, X = NH, Y = CH_2, Z = H, R = Et;
H8: W = CH_2, X = NH, Y = ($CH_2)_2$, Z = H, R = Et;

Fig. 2. Ferrocene-bisphosphonate hybrids **(H1-H8)**.

The formation of the ferrocenylaminobisphosphonic acid hybrids was confirmed by the peak of the methylene proton linked to ferrocene and amine bond (Fc**CH_2**NH) observed around 3.5 to 4.0 ppm and disappearance of the aldehyde peak around 9.6 ppm in the proton NMR spectra. Likewise, In the ^{13}C NMR, the presence of the peaks of the carbon of the methylene groups linked to the amine functional group, (Fc**C**H_2NH**C**H_2) around 47.0 ppm also confirmed their formation. As expected, there was no significant shift in the position of phosphorus in the ^{31}P NMR spectra of the hybrid, as the point of conjugation of the ferrocene and bisphosphonate moieties is far from the phosphorus atoms of the bisphosphonates. We also confirmed the isolation of this class of hybrids from their IR stretchings; For **H3**, the N—H stretching of the amine bond was seen at 3234 cm^{-1}, C—H stretching for ferrocene at 3088 cm^{-1}, P═O at 1003 cm^{-1} and P-OH of the bisphosphonate at 1175 and P—C at 812.[54]

*2.1.3.2. Synthesis of ferrocenylamidobisphosphonate (**H4-H6**).* Hybrids **H4-H6** were synthesized by amide bond formation between ferrocene carboxylic acids and aminobisphosphonates (Scheme 2). This was achieved by direct coupling of the ferrocenyl carboxylic acids (**F1**, **F2** and **F3)** with tetraethyl-3-aminopropane-1-1-bisphosphonate (**B5)** using a 50 % solution of propylphosphonic anhydride (T3P) (coupling agent) in ethyl acetate in the presence of pyridine (base) to form **H4**, **H5** and **H6**, respectively. Pyridine was selected because of its reported high yield with T3P in literature.[44] The crude product obtained was purified by column chromatography on silica gel with ethyl acetate: methanol (90:10) as eluent. Use of Dicyclohexyl carbodiimide (DCC), a coupling agents and N- hydroxysuccinimide in place of T3P, in this reaction also afforded the product though the crude was difficult to purify. The synthesis of these hybrids was confirmed by the presence of the methylene protons linked to the NH of the amide bond (CONH**CH_2**) at around 3.5 ppm in the proton NMR spectra. For the carbon ^{13}CNMR, the shift of the **CO**OH peak in the ferrocenylcarboxylic acids from around 181 ppm to around 170 ppm of **CO**NH peak confirms the formation of the amide bond in these hybrids. In ^{31}P NMR. there was no significant change in the chemical shift of the phosphorus peak in the hybrid compound compared to tetraethyl-3-aminopropane-1-1-bisphosphonate (**B5)** as expected. The IR analysis also confirmed the formation of these hybrids. For **H5**, the N—H stretching of the amide bond was seen at 3298 cm^{-1}, C—H stretching for ferrocene at 3088, CH_2 antisymmetric and symmetric bonds at 2929 and 2986 respectively, C═O bond for the amide at 1641. Other bands observed include 1443 for N—H of amide, 1386 for C—N of amide, 1362 for CH_2 twisting. In addition, the following bands were observed for the bisphosphonate moiety of the hybrid; 1016 for P═O bond and 793 for the P—C bond. The IR bands observed and reported were similar to the ones reported in literature.[54,55] The HRMS also confirmed the formation of the hybrids, giving [M+H] of 544.1322, 586.1776 and 600.1589 for **H4**, **H5 and H6,** respectively.

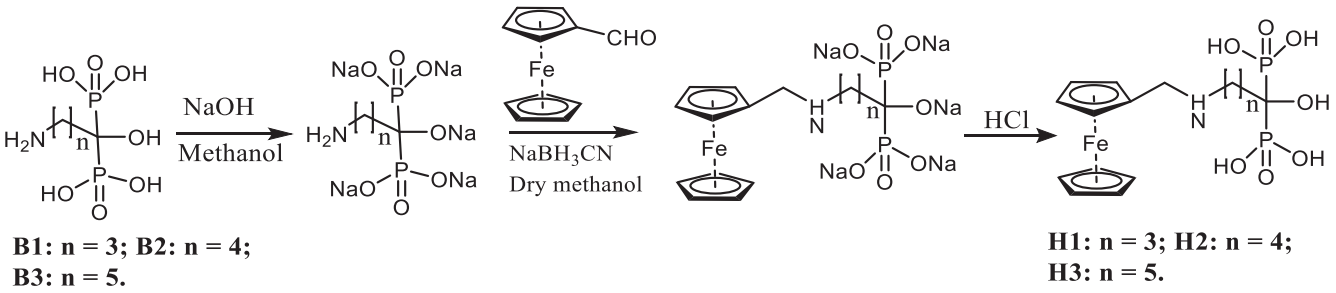

Scheme 1. Synthesis of ferrocenylaminobisphosphonic acids.

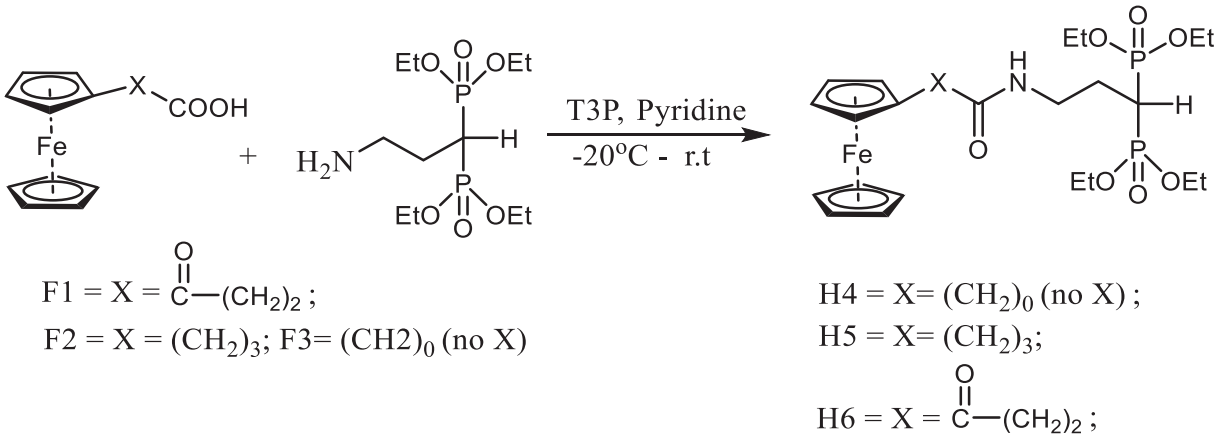

Scheme 2. Synthesis of ferrocenylamidobisphosphonates.

2.1.3.3. Synthesis of ferrocenylaminebisphosphonatesters. **H7** was prepared by the reaction of ferrocenylamine (**F5**) with tetraethylvinylidene phosphonate (**B4**) (Scheme 3). As an electron-deficient alkene, **B4** underwent conjugate addition of strong and mild nucleophiles, serving as a Michael addition acceptor in this reaction. The crude product obtained was rapidly purified to avoid *retro*-Michael reaction and **H7** was isolated in moderate yield and remained stable even after months of isolation. The formation of this hybrid was confirmed by a shift in the phosphorus peak from around 12.9 ppm of the bisphosphonate derivative **B4** to around 23.5 ppm in the hybrids in the 31P NMR. Furthermore, for the proton NMR the disappearance of the ethylenic hydrogen peak at 6.8 ppm in **B4** confirmed the isolation of the hybrid.

Furthermore, **H8** was synthesized by reductive amination of ferrocene carboxaldehyde (**F4**) with Tetraethyl-3-aminopropane-1-1-bisphosphonate ester (**B5**) in a one-pot synthesis in methanol solvent using $NaBH_3CN$ as the reducing agent (see Scheme 4). Attempts to synthesize **H8** by a two-step reaction of imine formation and further reduction with $NaBH_4$, resulted in low yields (28–30 %) of the product. The presence of the Fc**CH**$_2$NH peak at around 3.6 in **H8** confirmed the formation of the target product. The IR spectra showed a band at 3438 cm^{-1} for N—H of amine, 3088 cm^{-1} for CH of ferrocene, 1016 for P═O bond and 779 for P—C bond of bisphosphonate.

2.2. Cytotoxicity assays in human cancer cell lines

Table 1 shows the IC_{50} of the hybrids, **H1-H8**, ferrocene derivatives, **F1-F5** and bisphosphonate derivatives, **B1-B5** on lung (A549), cervical adenocarcinoma (HeLa) and normal murine fibroblast (NIH3T3) cell lines. Overall, the hybrids exhibited higher cytotoxicity on HeLa than A549 cells lines. Interestingly, minimal toxicity was observed on the non-cancerous NIH3T3 cell line compared to the parent compounds and the positive controls. The lead compound **H6** demonstrated twice the potency of cisplatin on A549 cells and was equivalent in potency to cisplatin on HeLa cells. The lead compound was also 5 times less toxic than cisplatin on the healthy cell line (NIH3T3).

Hybridization also demonstrated improved activity of the ferrocenylaminobisphosphonic acid hybrids (**H1-H3)** on HeLa cells but a loss in activity on A549 cells. **H1** exhibited cytotoxicity of IC_{50} = 29.01 μM while its parent compounds (B1 and F4) exhibited a cytotoxicity of IC_{50} = 48.03 and 133.2 μM respectively on HeLa cells. Likewise, **H2** exhibited cytotoxicity of IC_{50} = 22.44 μM while its parent compounds (B2 and F4) exhibited IC_{50} values of 46.61 and 133.2 μM respectively.

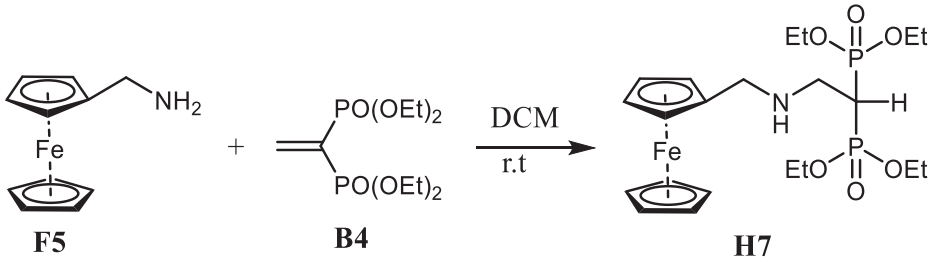

Scheme 3. Synthesis of ferrocenylaminebisphosphonatester, H7.

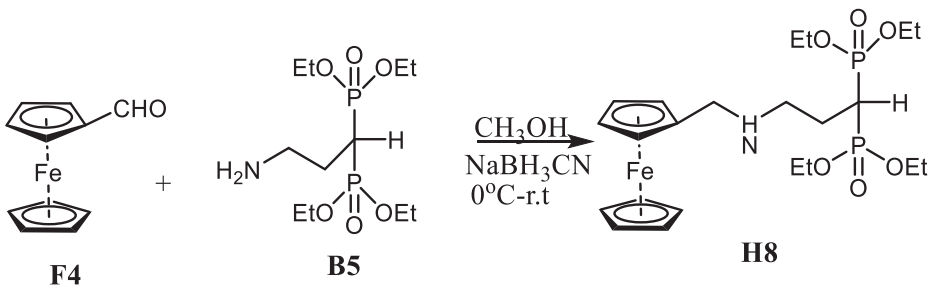

Scheme 4. Synthesis of ferrocenylaminebisphosphonate, H8.

Table 1
IC_{50} of Hybrids, **H1-H8**, Ferrocene derivatives, **F1-F5** and bisphosphonate derivatives, **B1-B5** on A549, HeLa and NIH3T3 cells.

	IC_{50}[a] (μM)		
	A549	**HeLa**	**NIH3T3**
CISPLATIN	58.25 ± 0.0390	15.10 ±2.10[b]	20.86 ± 0.0210
PTX	3.53 ± 0.0483	4.30 ± 0.0384	10.46 ± 0.0498
H1	87.93 ± 0.1298	29.01 ± 0.0272	116.64 ± 0.0104
H2	108.80 ± 0.0483	22.44 ± 0.0423	119.77 ± 0.0127
H3	97.72 ± 0.4423	24.38 ± 0.0282	-
H4	112.49 ± 0.0309	54.00 ± 0.0629	108.17 ± 0.0118
H5	39.71 ± 0.0604	75.36 ± 0.0462	57.69 ± 0.0671
H6	28.15 ± 0.0451	14.69 ± 0.0610	95.58 ± 0.0338
H7	82.19 ± 0.0579	51.48 ± 0.0676	16.91 ± 0.1125
H8	69.04 ± 0.0266	30.18 ± 0.0300	60.66 ± 0.0114
F1	1.73 ± 0.0726	139.32 ± 0.0567	25.61 ± 0.028
F2	152.2 ± 0.0400	32.40 ± 0.0446	26.10 ± 0.0341
F3	108.99 ± 0.0232	52.43 ± 0.0318	-
F4	135.28 ± 0.0699	133.22 ± 0.0512	41.31 ± 0.0884
F5	106.54 ± 0.0740	103.89 ± 0.0342	-
B1	27.53 ± 0.0569	48.03 ± 0.0335	13.65 ± 0.0314
B2	21.56 ± 0.0501	46.61 ± 0.0553	25.61 ± 0.0204
B3	36.74 ± 0.0332	62.19 ± 0.0573	-
B4	122.60 ± 0.0675	156.39 ± 0.0249	22.16 ± 0.0759
B5	22.17 ± 0.0319	29.56 ± 0.0640	-
C1	45.59 ± 0.0461 μg/ml	19.52 ± 0.0357 μg/ml	25.00 ± 0.0024 μg/ml
C2	7.30 ± 0.0335 μg/ml	12.45 ± 0.0632 μg/ml	-

[a]Compound concentration that is required to inhibit cell proliferation by 50% after 48 h treatment. Data are expressed as the mean ± SEM from the concentration–response curves of three experiments.
[b]Data taken from Refs. 59 and 60. **C1** = equimolar combination of 4-ferrocenylbutanoic acid and tetraethyl-3-aminopropane-1-1-bisphosphonate; **C2** = equimolar combination of ferrocene carboxaldehyde and (4-amino-1-hydroxy-1-phosphobutyl) phosphonate. Good activity (red), medium activity (purple), poor activity (blue), safe (green), moderately safe (ash) etc

The cytotoxic activity of **H3** was 24.38 μM on HeLa cells while their parent compounds (B3 and F4) exhibited IC_{50} values of 62.19 μM and 133.2 μM respectively (Fig 3).

The activity of **H1**, **H2** and **H3** on HeLa cells demonstrated similar activity to cisplatin (15.10 μM) and was lower than that of paclitaxel (4.30 μM). Furthermore, **H1**, **H2** and **H3** also showed activity values of 87.98, 108.80 and 97.72 μM respectively on A549 cells, while their derivatives (B1, B2, B3 and F4) exhibited IC_{50} values of 27.53, 21.56, 36.74 and 135.28 μM respectively with cisplatin and PTX having activities of 58.25 and 3.53 μM respectively.

For tetraethylferrocenylamidobisphsphonates (**H4-H5)** hybridization resulted in a loss of activity on A549 and HeLa cells, except for **H6**

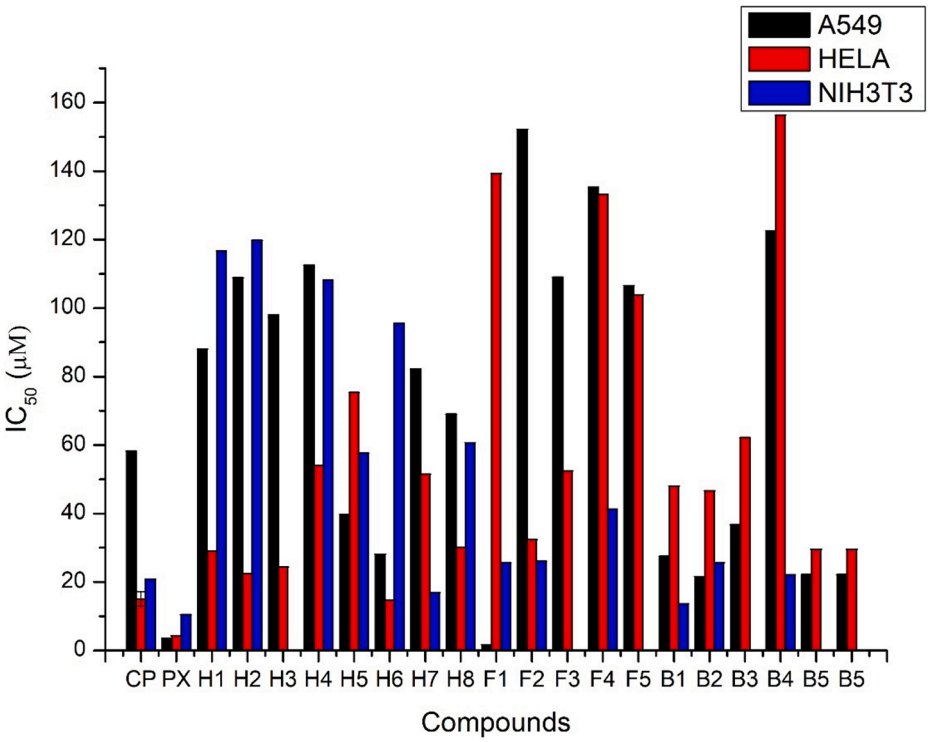

Fig. 3. *In vitro* cytotoxicity of Hybrid compounds (H1-H8), ferrocene derivatives (F1-F5), and bisphosphonate derivatives (B1-B5) on A549, HeLa and NIH3T3 cell lines. CP = Cisplatin. PX = Paclitaxel. Cytotoxicity on NIH3T3 was not evaluated for compounds with no third bar in the chart. Error bars fall within the graph, were not observed.

where an improved activity was recorded specifically on HeLa cells. Hybrids **H4**, **H5** and **H6** were cytotoxic to A549 cells (IC_{50} = 112.49, 39.71 and 28.15 μM respectively) and their pharmacophores (F1, F2 and F3 and B5) had IC_{50} values of 108.99 152.20, 1.73 and 22.17 μM respectively on A549 cells. **H4**, **H5** and **H6** also provided cytotoxic activity on HeLa cells (IC_{50} of 54.00, 14.69 μM and 75.36 μM respectively) with their pharmacophores (F1, F2 F3 and B5) exhibiting activities of IC_{50} = 52.43 32.40, 139.32**,** and 29.56 μM**,** respectively.

For tetraethylferrocenylaminobisphosphonates, **H7-H8**, hybridization resulted in improvement in activity for **H7** on A549 and HeLa cells but a loss in activity for **H8** on both cell lines. **H7** exhibited cytotoxicity activity of IC_{50} = 82.19 μM while its parent compounds (**F5** and **B4)** exhibited cytotoxicity activity of IC_{50} = 106. 54 and 122.60 μM respectively on A549 cells. **H7** also exhibited cytotoxicity activity of 51.48 μM on HeLa cells with its pharmacophores (**F5** and **B4)** showing IC_{50} cytotoxicity of 103.89 and 156.39 μM, respectively. On the other hand, **H8** exhibited IC_{50} cytotoxicity of 69.04 μM while its pharmacophores, **F4** and **B5** exhibited IC_{50} cytotoxicity of 108.99 and 22.17 μM respectively on A549 cells. **H8** also displayed IC_{50} cytotoxicity of 30.18 μM with its pharmacophores (**F4** and **B5)** exhibiting cytotoxicity of IC_{50} = 135.22 μM and 29.56 μM respectively on HeLa cells.

Some of the ferrocene and bisphosphonate parent compounds exhibited high cytotoxic activity. Importantly, 4-ferrocenyl-4-oxo-butanoic acid (**F1)** exhibited an activity of 1.73 μM on A549 cells. This agrees with earlier reports on the cytotoxicity of ferrocenyl derivatives on lung cancer cell lines. Corry *et al.* reported several *N*- [*ortho*-ferrocenyl)benzoyl] dipeptide ethyl esters which exhibited good anticancer activity (5.3–21 μM) against lung carcinoma cell line, H1299.[56] In contrast, the activity of F1 on HeLa cells was 139.32 μM, showing that its activity on A549 cells may be selective. Furthermore, the toxicity of **F1 (**IC_{50} = 25.61 μM) on the NIH3T3 cell line when compared to that of PTX (10.46 μM) shows that it is safer than PTX. Other parent compounds that exhibited superior cytotoxicity were **B1**, **B2** and **B3** which had activities of 27.53, 21.56 and 36.74 μM respectively on A549 cells. **F2** and **B5** also exhibited activities of 32.40 and 29.56 μM on HeLa cells.

There was a remarkable reduction in the toxicity of the novel ferrocene-bisphosphonate hybrids on N1H3T3 cells (IC_{50} = 57.6–119.77 μM) as compared to their toxicity on HeLa cells (14.69–75.36 μM). PTX and cisplatin gave IC_{50} of 10.46 and 20.86 μM respectively on NIH3T3 (Fig 3). The low toxicity obtained for the hybrid compounds agrees with other reports on the toxicity of ferrocene. The first ferrocene compound used in clinical practice, the sodium salt of *o*-carboxybenzoyl ferrocene showed low toxicity of LD_{50} = 60 $mgkg^{-1}$ *in vivo*.[57] Sathyadevi et al.,[58] also reported **a** reduction in the toxicity of ferrocene (Schiff base)-Cu complex on NIH3T3 (420–455 μM) as compared to its toxicity on HeLa cells (130–212 μM).

An increase in the alkyl chain length from n = 2, (**H7**) to n = 3, (**H8**) resulted in **a** superior activity of the ferrocene-bisphosphonate hybrids linked by amine**.** This conforms to a previously published study by Wang et al. that showed an increase in alkyl chain length resulting in increased anticancer activity.[14] In addition, **H4** and **H7**, which have the same alkyl chain (n = 2) but different type**s** of linkers showed variation in activity. **H7,** linked by an amine exhibited higher cytotoxicity on A549 cell and HeLa cells than **H4** linked by an amide. The reason for the higher cytotoxicity of the amide is unknown. Furthermore, the replacement of a methyl group (CH_2) in **H5** with a keto group (C═O) in **H6** resulted in an improvement of the activity of the hybrid.

There is debate on the effectiveness of combination drug therapy over hybrid drug compounds. Therefore, the anticancer activity of a 1:1 mol combination of selected pharmacophores was compared with their hybrids (Fig 4). An **F2** and **B5** combination (**C1)** provided an activity of 45.59 μg/ml and 19.52 μg/ml on A549 and HeLa cells respectively while **H5**, a hybrid of both provided an activity value of 23.24 μg/ml (39.71 μM) and 44.41 μg/ml (75.36 μM) on A549 and HeLa cell lines, respectively. This meant that while the hybrid (**H5)** may be preferred in the treatment of patients with lung cancer, the combination (**C1)** may be considered instead for the treatment of cervical cancer. Likewise, a combination of **F4** and **B1 (C2)** provided an IC_{50} activity of 7.53 μg/ml

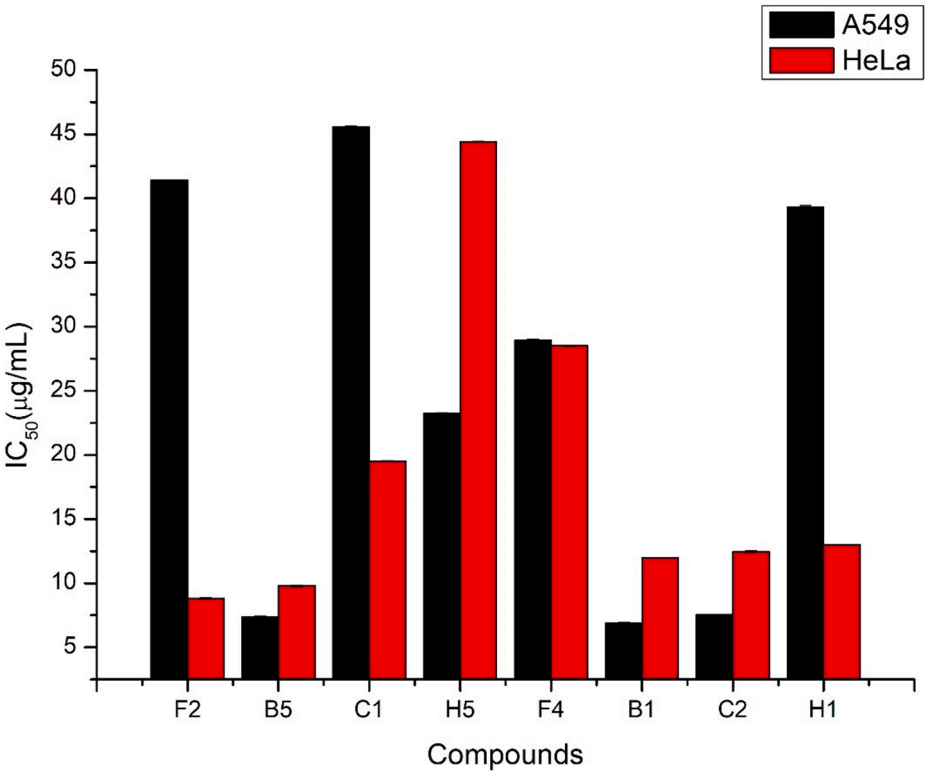

Fig 4. Comparison of the effect of combination therapy with hybridization on HeLa cell line. **C1** = equimolar combination of **F2** and **B5**. **H5** = hybrid of **F2** and **B5.** **C2** = equimolar combination of **F4** and **B1**. **H1** = hybrid of **F4** and **B1.** Error bars fall within the graph, were not observed.

and 12.45 μg/ml, respectively on A549 and HeLa cells while the hybrid **H1** provided an IC_{50} value of 39.31 μg/ml (87.93 μM) and 12.97 μg/ml (29.01 μM), respectively. In this instance, a combination is preferred over hybridization.

Furthermore, previous studies have reported the important therapeutic targets in the treatment of lung cancer[61] and cervical cancer[62]. In the present study, molecular docking studies were used to profile the binding affinity of compounds **F1** and **H6** for Src homologous and collagen (SHC) SH2-binding protein 1 (SHCBP1), as well as Signal transducer and activator of transcription 3 (STAT3), which are key therapeutic targets in A549. Compound **H6** was additionally docked against important drug targets in the HeLa cell line (Caspase-3, Mucosal addressin cell adhesion molecule 1(MAdCAM-1) and cellular tumor antigen p53). The docking scores (Kcal/mol) of the studied compounds against the different drug targets are tabulated in Tables 2 and 3.

Docking analysis of the ligands against the A549 cell line revealed that **F1** showed a binding free energy of −2.411 and −3.689 Kcal/mol with SHCBP1 and STAT3, respectively. Similarly, the complex formed between **H6** with each of the SHCBP1 and STAT3 proteins released the binding energy of −0.993 and −4.112 kcal/mol, respectively.

Table 2
Binding energy (Kcal/mol) of the docked compounds, **F1** and **H6** against A549 proteins along with their H-bonds interaction.

Ligands	Target	PDBID	Dock score (Kcal/mol)	No of H-bonds	Residues
F1	SHCBP1	1TCE	−2.411	1	LEU55
	STAT3	6QHD	−3.689	1	CYS712
H6	SHCBP1	1TCE	−0.993	2	$ASP58^2$
	STAT3	6QHD	−4.112	2	GLU638, THR714
Carboplatin	SHCBP1	1TCE	−1.792	1	ASP58
	STAT3	6QHD	−4.004	2	CYS712, PHE710

Table 3
Binding energy (Kcal/mol) of **H6** and Carboplatin against HeLa cell line proteins along with their H-bonds interaction.

Ligands	Targets	PDBID	Dock score (Kca/mol)	No of H-bonds	Residues
H6	MAdCAM-1	4HD9	−5.519	3	$VAL56^2$, $ARG70^1$
	Caspase-3	3DEI	−2.386	1	GLU123
	Cellular antigen	6VTC	−4.620	3	ASP165, $VAL163^2$
Carboplatin	MAdCAM-1	4HD9	−3.313	3	$ARG60^2$, SER63
	Caspase-3	3DEI	−3.478	3	$GLY122^2$, OCS163
	Cellular antigen	6VTC	−3.066	1	ARG109

Furthermore, the binding free energy of **H6** against STAT3 was comparable with that of the reference anti-cancer drug, carboplatin, whose binding energy was −0.108 less. Wang et al.[61] have studied the role of SHCBP1 in upregulating apoptosis of lung cancer. They concluded that this protein may be an effective novel therapeutic target against the disease. Therefore, the free binding energy of compounds **F1** in this present study may suggest its capacity to disrupt the SHCBP1pathway. Similarly, the stronger affinity of **H6** for STAT3 might indicate the ability to induce cell death in lung cancer cells thereby, inhibiting the activation of STAT3.

As contained in Table 3, H6 showed a stronger binding affinity for the Mucosal Addressin Cell Adhesion and Cellular antigen receptors, releasing binding energy of −2.206 and −1.554 Kcal/mol respectively, more than the reference compound, carboplatin. The weaker affinity (-2.386 Kcal/mol) of **H6** for the caspase-3 protein suggests that the compound might have inhibited HeLa cell lines by disrupting other pathways different from apoptosis which is induced by caspase 3.

Fig. 5 presents the molecular docking interaction of compounds **F1** and **H6**. **F1** formed one hydrogen bond interaction with the amino acid LEU55 of the SHCBP1 protein (Fig. 5a). Moreover, the protein–ligand interaction of STAT3 (6QHD) with **H6** formed two hydrogen bonds, involving the GLU638 and THR714 residues (Fig 5b). Similarly, Fig. 5c illustrates the interaction between MAdCAM-1 and **H6** where three hydrogen bonds involving VAL56, and ARG70 participated. In the like manner, the ASP165, and VAL163 residues of the cellular antigen (6VTC) formed three hydrogen bonds with compound **H6**. The hydrogen bond is a key factor that plays a role in influencing the binding effect between the protein–ligand complexes. A hydrogen bond distance of >3.5 Angstrom can decrease the stability of the affinity between an enzyme and its substrate.[63] Interestingly, the distances observed in our docking complexes were within the required cut-off. This indicates that the compounds may have a strong affinity and stability for driving potent binding with their respective targets.

3. Conclusions

Hybridization of ferrocene and bisphosphonate moieties yielded compounds that have the potential to act as anticancer agents. The nature of the linker, chain length, and solubility of the various hybrids influenced their activity. All the hybrids, except **H5**, exhibited higher cytotoxicity on HeLa cells than on A549 cells. Most hybrids also exhibited higher cytotoxicity than their individual pharmacophores. An increase in alkyl chain length resulted in superior activity among the tetraethylferrocenylaminobisphosphonates. Of all the reported hybrids, **H6** exhibited the best activity that was superior to the activity of cisplatin on A549 and HeLa cells**.** Interestingly, most hybrids also exhibited low cytotoxicity on NIH3T3 cells compared with PTX and cisplatin suggesting that these compounds may be a safer option over PTX and cisplatin for chemotherapy. In addition, **F1**, a ferrocene derivative, exhibited outstanding and highly selective activity on A549 cells. Its activity was superior to that of PTX and cisplatin on A549 cell lines. In addition, an equimolar combination, of selected pharmacophores exhibited higher cytotoxicity than their hybrids. This means that medicinal chemists have many factors to consider before proposing hybrid compounds as potential drug candidates. The docking result further revealed that the observed activity of **FI** could be due to inhibition of STAT3 signalling and **H6** might have inhibited HeLa cell lines by disrupting other pathways different from apoptosis. Finally, the *in silico* study was in support of the empirical investigation which showed high cytotoxicity of **F1** on A549 cell lines, and of **H6** on both A549 and HeLa cell lines. The impact of activation/inhibition of STAT3 enzymes predicted by molecular docking will be assessed in future studies.

4. Experimental

4.1. General information

Compounds, ferrocene carboxaldehyde, **F4** (98%), ferrocene carboxylic acid (96%) **F3**, 4 aminobutyric acid (99%), 5 aminovaleric acid (99%) and 6-aminocarproic acid (99%) were purchased from Sigma-Aldrich- South Africa and were used as received. Methanol was dried over potassium hydroxide and stored over molecular sieves for use. Dichloromethane was dried over silica gel. Reactions were performed under nitrogen atmosphere except where otherwise stated. ^{1}H NMR. ^{13}C {^{1}H} NMR and ^{31}P {^{1}H} NMR spectra were recorded on a Bruker Ultrashield 400^{1}H NMR 400.17 MHz, ^{13}C {^{1}H} NMR 100.62 MHz and ^{31}P {^{1}H} NMR 161.99 MHz) and 500 ^{1}H NMR 500.13 MHz, ^{13}C {^{1}H} NMR 125.75 MHz and ^{31}P {^{1}H} NMR 202.46 MHz) in D_2O and $CDCl_3$ as specified at room temperature. HRMS (ESI) spectra were recorded on a waters synapt G2 spectrometer. Fourier transform infrared spectroscopy spectra were obtained from Brucker FTIR Alpha spectrometer.

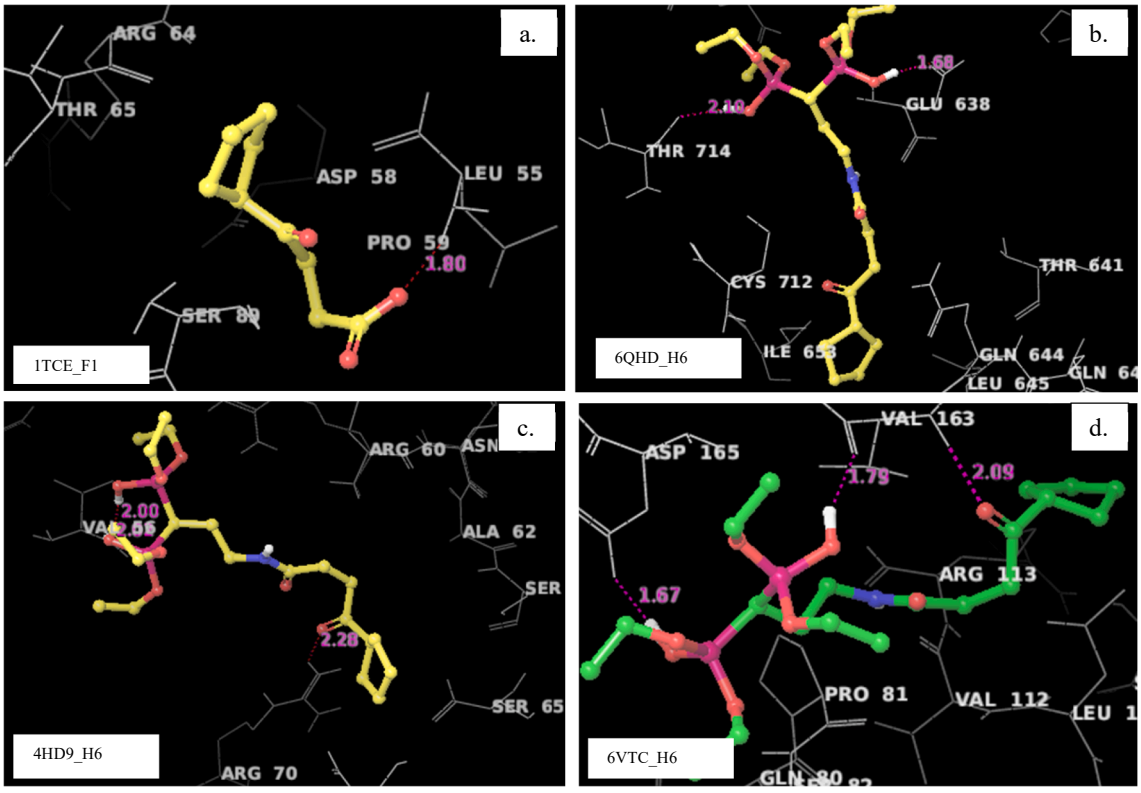

Fig. 5. Molecular docking interactions for compounds **F1** and **H6**. Fig. 5a-d shows the interaction between the complexes with stronger affinity than the known anticancer drug (carboplatin).

4.2. General method for the preparation of ferrocenylaminobisphosphonic acid (H1-H3) hybrids

The aminobisphosphonic acid was crushed and added to a methanol solution containing NaOH. The solution was stirred at 20–40 °C until the bisphosphonates dissolved completely. Ferrocene carboxaldehyde in methanol was added slowly while stirring the reaction mixture, followed by the dropwise addition of 4 equivalents of sodium cyanoborohydride ($NaBH_3CN$) or $NaBH_4$. The reaction was stirred for 48 h (h) at room temperature (r.t). The pH of the reaction mixture was adjusted to 2 and the resulting solution was allowed to age for 24 h at a temp of 0 – 5 °C. The resulting precipitate was filtrated and washed with cold water and 95% ethanol to yield the expected product.

4.2.1. Synthesis of 4-(ferrocenylmethyleneamino)-1-1-hydroxybutylidene-1-1-bisphosphonic acid, HI

Compound **H1** was synthesized using 0.20 g (0.8 mmol) of ((4-amino-1-hydroxy-1-phosphobutyl) phosphonate), **B1**, 0.34 g (1.6 mmol) of ferrocene carboxaldehyde, **F4**, 0.03 g (0.8 mmol) of NaOH and 0.20 g (3.2 mmol) of sodium cyanoborohydride ($NaBH_3CN$). Yield: 0.24 g (67%), colour: brown (solid), melting point: >180 °C (decomposed), ^{1}H NMR (500 MHz, D_2O): δ (ppm) 1.90 (s, br, 4H, $CH_2\underline{CH_2CH_2}C(P(O)(OH)_2)_2OH$), 2.95 (s, br, 2H, $NH\underline{CH_2}CH_2$), 4.02 (s, br, 2H, $Cp\underline{CH_2}NH$), 4.22 (s, 5H, Cp), 4.28 (s, br, 2H, subst. Cp), 4.37 (s, br, 2H, subst Cp). ^{31}P {^{1}H} (202 MHz, D_2O): δ 17.92. ^{13}C (126 MHz, D_2O): δ 21.07 (t, ^3Jcp = 10.10, CH_2 $\underline{C}H_2CH_2$), δ 30.74 ($CH_2\underline{C}H_2C(P(O)(OH)_2)_2OH$), δ 47.09 ($NH\underline{C}H_2CH_2$), -δ 47.28 ($Cp\underline{C}H_2CH_2$), δ 69.28 (Unsubst. Cp), δ 69.92 (Cp subst.), δ 70.46 (Cp subst.), δ 73.51 (t, ^1Jcp = 216.14, $CH_2\underline{C}(P(O)(OH)_2)_2OH$), δ 76.19 (Cp quart). HRMS (ESI^+): calcd *m/z*: 414.0323 $[M+H\text{-}2OH]^+$; found: 414.0366 $[M+H\text{-}2OH]^+$ [64]

4.2.2. Synthesis of 5-(ferrocenylmethyleneamino)-1-1-hydroxypentylidene-1-1-bisphosphonic acid, H2

Compound **H2** was synthesized with of ferrocene carboxaldehyde 0.48 g (1.82 mmol) of ((5-amino-1-hydroxy-1-phosphopentyl) phosphonate), **B2,** 0.39 g (1.82 mmol) of ferrocene carboxaldehyde, **F4**, 0.07 g (1.82 mmol) of NaOH and 0.46 g (7.28 mmol) of $NaBH_3CN$. Yield: 0.46 g (55%), colour: brown (solid), melting point: >180 °C (decomposed). ^{1}H NMR (500 MHz, D_2O): δ (ppm) 1.54 (s, br, 4H, CH_2 $\underline{CH_2CH_2}CH_2$) 1.82 (s, br, 2H, $\underline{CH_2}C(P(O)(OH)_2)_2OH$), 2.92 (s, br, 2H, $NH\underline{CH_2}CH_2$), 3.97 (s, br, 2H, $Fc\underline{CH_2}NH$), 4.17 (s, br, 4H, Cp), 4.23 (s, br, 2H, subst. Cp), 4.31 (s, br, 2H, subst Cp). ^{31}P {^{1}H} (202 MHz, D_2O): δ 18.20. ^{13}C (101 MHz, D_2O): δ 26.09 ($CH_2\underline{CH_2}$ $\underline{CH_2}CH_2$), δ 32.91($CH_2\underline{C}$(P(O)$(OH)_2)_2OH$), δ 46.16 ($NH\underline{C}H_2CH_2$), δ 47.13 ($Cp\underline{C}H_2NH$), δ 68.94 (Cp), δ 69.62 (Cp subst.), δ 70.15 (Cp subst.), δ 75.81 ($CH_2\underline{C}(P(O)(OH)_2)_2OH$). HRMS ($ESI^+$): calcd *m/z*: 381.0793 $[M+H—P(OH)_3]$; found: 381.0790 $[M+H—P(OH)_3]$.

4.2.3. Synthesis of 6-(ferrocenylmethyleneamino)-1-1-hydroxyhexylidene-1-1- bisphosphonic acid, H3

Compound **H3** was synthesized with 0.64 g (2.3 mmol) of ((6-amino-1-hydroxy-1-phosphohexyl) phosphonate), **B3**, 0.49 g (2.3 mmol) of ferrocene carboxaldehyde, **F4**, 0.09 g (2.3 mmol) of NaOH and 0.58 g (9.2 mmol) of $NaBH_3CN$. Yield: 0.64 g (59%), colour: brown (solid), melting point: >180 °C (decomposed). ^{1}H NMR (400 MHz, D_20): δ (ppm) 1.11 (m, J = 6.8 Hz 2H, $CH_2\underline{CH_2}CH_2$), 1.39 (m, J = 7.2 Hz, 4H, $CH_2\mathbf{CH_2}CH_2\mathbf{CH_2}CH_2$), 1.71-1.64 (m, J = 12.8 Hz, 2H, $CH_2\mathbf{CH_2}C(P(O)(OH)_2)_2OH$), 2.47–2.41 (q, J = 7.4 Hz, 2H, $CH_2NH\mathbf{CH_2}CH_2$), 3.35 (s, 2H, $Fc\mathbf{CH_2}NHCH_2$), 4.03 (s, 2H, subst Cp), 4.12 (s, 2H,subst. Cp), 4.06 (s, 5H, Cp), ^{31}P {^{1}H} (162 MHz, D_2O): δ 18.81. ^{13}C (126 MHz, D_2O): δ 22.93 (d, Jcp = 10.10, $CH_2\underline{CH_2}CH_2$), 25.15 ($CH_2\underline{CH_2}CH_2$), 26.39 ($CH_2\underline{CH_2}CH_2$), δ 33.34 ($CH_2\underline{CH_2}C(P(O)(OH)_2)_2OH$), δ 46.41 ($NH\underline{CH_2}CH_2$), δ 47.04 ($Cp\underline{CH_2}NH$), δ 69.21 (Cp), δ 69.84 (Cp subst.), δ 70.43 (Cp subst.), δ 73.99 (t, ^1Jcp = 218.16 Hz, $CH_2\underline{C}(P(O)(OH)_2)_2OH$), δ 76.12 (Cp quart-C). HRMS (ESI^+): calcd *m/z*: 476.0690 $[M+H]^+$; found: 476.0663 $[M+H]^+$

4.3. General procedure for the preparation of tetraethylferrocenylamidobisphosphonates (H4-H6)

Ferrocenecarboxylic acid, tetraethyl-3-aminopropane-1-1 bisphosphonate and pyridine were added in ethyl acetate and stirred. The reaction mixture was cooled to −10 °C. T3P solution (in 50 wt% EtOAC) was added dropwise to maintain an internal temperature below 0 °C. The resulting homogeneous solution was stirred at 0 °C for 4 h and then at r.t for 16 h. The reaction mixture was then washed with saturated Na_2CO_3, 0.1 M HCl and again with Na_2CO_3. The organic extracts were dried over $MgSO_4$ and concentrated in vacuo to give a yellow oil. The crude was purified by column chromatography using ethyl acetate: methanol (95%:5%) to get the expected product.

4.3.1. Tetraethyl (3-ferrocenylamidopropane-1-1-diyl) bis(phosphonate) H4

Compound **H4** was synthesized using 0.36 g (1.56 mmol, 1 eq) of ferrocenecarboxylic acid, **F3**, 1.03 g (3.12 mmol, 2 eq) of tetraethyl −3 -amino-propane-1, 1 bisphosphonate, **B5** and 0.49 ml (0.49 g, 6.24 mmol, 4 eq) of pyridine, 10 ml of ethyl acetate and 2.32 ml of T3P solution (50 wt% EtOAC, 1.24 g, 3.9 mmol, 2.5 eq). Yield: 0.56 g (66%), colour: brown (oil)**.** ^{1}H NMR (500 MHz, $CDCl_3$): δ (ppm) 7.03 (s, br 1H, $\underline{NH}$) δ 4.73 (s, br, 2H, subst. Cp), 4.64 (s, br, 2H, subst Cp), δ 4.16 (s, br, 12H, $O\underline{CH_2}CH_3$; Cp), 3.56 (br, s, 2H, $CONH\underline{CH_2}$), 2.37 (t, J = 23.5 Hz, 1H, $\underline{CH}(PO(OCH_3CH_2)_2)_2$), 2.02 (s, br, 2H, $\underline{CH_2}CH(PO(OCH_3CH_2)_2)_2$), 1.32 (s, br, 12H, $OCH_2\underline{CH_3}$). ^{31}P {^{1}H} (202 MHz, $CDCl_3$): δ 23.73. ^{13}C (126 MHz, $CDCl_3$): δ 16.37 (d, ^3Jcp = 6.1, $OCH_2\underline{C}H_3$), δ 25.0 (t, ^2Jcp = 8.1, $\underline{CH_2}CH(PO(OCH_3CH_2)_2)_2$), δ 35.0 (t, ^1Jcp = 214.1, $CH_2CH(PO(OCH_3CH_2)_2)_2$), δ 38.80 (t, ^3Jcp = 12.1, $CONH\underline{C}H_2$), δ 62.8 (t, ^2Jcp = 12.1, $O\underline{C}H_2CH_3$), δ 68.2 (CH-subst. Cp), δ 69.7 (Cp unsubst.), δ 70.3 (CH-subst. Cp), 170.5 ($\underline{C}ONH$). HRMS (ESI^+): calcd *m/z*: 544.1316 $[M+H]^+$; found: 544.1322 $[M+H]^+$

4.3.2. Tetraethyl (3-(4-ferrocenylbutanamido)propane-1-1-diyl)bis (phosphonate) H5

Compound **H5** was synthesized using 0.16 g (0.6 mmol, 1 eq) of ferrocenebutanoic acid, **F2**, 0.4 g (1.2 mmol, 2 eq) of tetraethyl −3 -amino-propane-1, 1 bisphosphonate, **B5** and 0.19 ml (0.19 g, 2.4 mmol, 4 eq) of pyridine, 5 ml of ethyl acetate and 0.9 ml of T3P solution (50 wt % EtOAC, 0.48 g, 1.5 mmol, 2.5 eq). Yield: 0.24 g (69%), colour: yellow (oil). ^{1}H NMR (500 MHz, $CDCl_3$): δ (ppm) 1.33 (t, J = 7.1 Hz, 12H, $OCH_2\underline{CH_3}$), 1.80 (m, J = 7.4 Hz, 2H, $FcCH_2\underline{CH_2}CH_2$), 2.12 (m, 4H, $Fc\underline{CH_2}$; $\underline{CH_2}CHPO(OCH3CH_2)$, 2.32 (m, J = 7.5 Hz, 3H, $\underline{CH_2}CONH$; $(CH_2\underline{CH}(PO(OCH_3CH_2)_2)_2$, 3.43 (q, J = 6.0 Hz, 2H,$CONH\underline{CH_2}$), δ 4.03 (s, br, 2H, subst Cp), δ 4.05 (s, br, 2H, subst. Cp), δ 4.09 (s, 5H, Cp), δ 4.16 (q, J = 7.2 Hz, 8H, $O\underline{CH_2}CH_3$), δ 6.52 (s, br 1H, $\underline{NH}$)**.** ^{31}P {^{1}H} (202 MHz, $CDCl_3$): δ 23.5. ^{13}C (126 MHz, $CDCl_3$): δ 16.4 (d, ^3Jcp = 10.10, $OCH_2\underline{C}H_3$), δ 25.1 ($FcCH_2\underline{C}H_2CH_2$), δ 26.9 ($Fc\underline{C}H_2CH_2$), δ 29.1 ($CONHCH_2\underline{C}H_2CH$), δ 34.8 ($CH_2CH(PO(OCH_3CH_2)_2)_2$), δ 36.3 ($\underline{C}H_2CONH$) δ 38.7 (t, ^3Jcp = 10.8, $CONH\underline{C}H_2$), δ 62.8 (t, ^2Jcp = 12.0 $O\underline{C}H_2CH_3$), δ 67.3 (CH-subst. Cp), δ 68.2 (CH-subst. Cp), δ 68.7 (CH-Cp), δ 173.0 ($\underline{C}ONH$). HRMS (ESI^+): calcd *m/z*: 586.1786 $[M+H]^+$; found: 586.1776 $[M+H]^+$.

4.3.3. Tetraethyl (3-(4-oxo-4-ferrocenylbutanamido)propane-1-1-diyl bis (phosphonate) H6

Compound **H6** was synthesized with 0.30 g (1.0 mmol, 1 eq) of ferrocene ketobutanoic acid, **F1**, 0.66 g (2.0 mmol, 2 eq) of tetraethyl −3 -amino-propane-1, 1 bisphosphonate, 0.24 ml (0.24 g, 3 mmol, 3 eq) of pyridine, 10 ml of ethyl acetate and 1.5 ml of T3P solution (50 wt% EtOAC, 0.80 g, 2.5 mmol, 2.5 eq). Yield: 0.35 g (58%), colour: brown (oil) ^{1}H NMR (500 MHz, $CDCl_3$: δ (ppm) 1.33 (m, J = 1.5 Hz, 5.5 Hz, 12H, $OCH_2\mathbf{CH_3}$), 2.14 (m, J = 4 Hz,7Hz, 2H, **(**$\underline{CH_2}CHPO(OCH_3CH_2)$), 2.41 (tt, J = 2 Hz,5 Hz, 1H, **(**$CH_2\underline{CH}PO(OCH_3CH_2)$)**)**, 2.53 (t, 2H, J = 7, $\underline{CH_2}CONH$), 3.09 (t, J = 7 Hz, 2H, $FcCO\mathbf{C}\underline{H_2}CH_2$), 3.46 (q, J = 13 Hz, 2H, $CONHCH_2$), 4.16(q, J = 7 Hz, 8H, $OCH_2\underline{CH_3}$), 4.20 (s, 5H, Cp), 4.47 (t, J

= 2 Hz, 2H, subst. Cp), 4.78 (t, *J* = 2 Hz, 2H, subst. Cp), 6.6 (s, 1H, NH) ^{31}P {^{1}H} (202 MHz, $CDCl_3$): δ 23.52. ^{13}C (126 MHz, $CDCl_3$): *δ* 16.4 (d, ^{3}Jcp = 9.4 Hz, $OCH_2\underline{C}H_3$), *δ* 25.2 ($\underline{C}H_2CH_2CONH$), *δ* 30.1 (d, ^{2}Jcp = 93.6 $\underline{C}H_2CH$), *δ* 34.6 (t, ^{1}Jcp = 214, $CH_2\underline{C}H$), *δ* 34.9 ($FcCO\underline{C}H_2CH_2$), *δ* 38.7 (d, ^{3}Jcp = 11.31, $CONH\underline{C}H_2$), *δ* 62.7 ($O\underline{C}H_2CH_3$), *δ* 69.2 (C-subst. Cp), *δ* 69.9 (C-subst. Cp), *δ* 72.1 (C-subst. Cp), *δ* 78.6 (Quart-C), *δ* 172.4 ($CH_2\underline{C}ONHCH_2$), *δ* 202.8 ($Fc\underline{C}OCH_2$). HRMS (ESI^+): calcd *m/z*: 600.1578 $[M+H]^+$; found: 600.1589 $[M+H]^+$.

4.4. Synthesis of tetraethylferrocenylamidobisphosphonates (*H7-H8*)

4.4.1. Tetraethyl (2-(ferrocenylmethyleneamino) ethane-1-1-diyl bis (phosphonate) H7

A solution of TEVB (0.93 mmol, 0.28 g, 1 eq) in anhydrous DCM was treated with ferrocenylmethylene amine (0.93 mmol, 0.20 g, 1 eq) under a nitrogen atmosphere for 2 h at r.t. The solvent was thereafter removed with a rotary evaporator, and residue purified by column chromatography with ethyl acetate: methanol (95:5). Yield: 0.30 g (63%), colour: brown (oil). ^{1}H NMR (400 MHz, $CDCl_3$): *δ* (ppm) 1.35 (t, *Jcp* = 6.8 Hz, 6H, $O\underline{CH_2}CH_3$), 2.71 (tt, *Jcp* = 5.84 Hz, 11.76 Hz, 1H, $CH_2\underline{CH}(PO(O\underline{CH_3}CH_2)_2)_2$), 3.21 (dt, *Jcp* = 5.2 Hz, 16.4 Hz, 2H, $\underline{CH_2}CH(PO(O\underline{CH_3}CH_2)_2)_2$), 3.55 (s, 2H, $Fc\underline{CH_2}NH$), 4.06 (s, 2H, subst. Cp), 4.11 (s, 5H, Cp), 4.12 (s, 2H, subst. Cp), *δ* 4.16 (q, *Jcp* = 7.6 Hz, 8H, $O\underline{CH_2}CH_3$). 31P {1H} (202 MHz, CDCl3): δ 23.43. ^{13}C (126 MHz, $CDCl_3$): *δ* 16.41 (d, ^{3}Jcp = 9.94, $OCH_2\underline{C}H_3$), *δ* 36.62 (t, ^{1}Jcp = 209.4, $CH_2\underline{CH}(PO(O\underline{CH_3}CH_2)_2)_2$), *δ* 48.42 ($CH_2NH\underline{C}H_2$), *δ* 49.08 ($Fc\underline{C}H_2NHCH_2$), *δ* 62.8 (m, ^{2}Jcp = 9.53, $O\underline{C}H_2CH_3$), *δ* 68.4 (m, Fc-Carbon), *δ* 81.47 (quart. Carbon). HRMS (ESI^+): calcd *m/z*: 516.1367 $[M+H]^+$; found: 516.1359 $[M+H]^+$.

4.4.2. Synthesis of tetraethyl (3-ferrocenylmethylamino propane-1-1-diyl bis (phosphonate) *H8*

0.50 g (1.5 mmol) of tetraethyl −3 -amino-propane-1, 1 bisphosphonate, **B5** and 0.21 g (1.0 mmol) ferrocene carboxaldehyde, **F4**, were dissolved in dry methanol under hydrogen atmosphere and stirred, this was followed by the addition of 0.25 g of $NaBH_3CN$, which was previously dissolved in dry methanol in drops. The reaction was stirred for 5 h at r.t. 10 ml of 1 M NaOH was added, and the product was extracted using dichloromethane. The excess solvent was removed using a rotary evaporator and the product was purified by column chromatography on silica gel with ethylacetate and methanol in the ratio of 95:5. Yield: 0.44 g (83%), colour: brown (oil), ^{1}H NMR (500 MHz, $CDCl_3$): *δ* (ppm) 1.29 (t, *J* = 6.0 Hz, 12H, $OCH_2\underline{CH_3}$). *δ* 2.18 (t, *J* = 5.5 Hz,11 Hz, 2H, $\underline{CH_2}CH(PO(O\underline{CH_3}CH_2)_2)_2$), *δ* 2.59 (t, *J* = 24.5 Hz, 1H, $\underline{CH}(PO(O\underline{CH_3}CH_2)_2)_2$), *δ* 2.92 (br, s, 2H, $CH_2NH\underline{CH_2}$), *δ* 3.67 (s, 2H, $Cp\underline{CH_2}NHCH_2$), *δ* 4.13 (m, 15H, $O\underline{CH_2}CH_3$; Cp, subst Cp), *δ* 4.25 (s, br, 2H, subst Cp). ^{31}P {^{1}H} (202 MHz, $CDCl_3$): δ 23.38. ^{13}C (126 MHz, $CDCl_3$): *δ* 16.38 (d, ^{3}Jcp = 10.1, $OCH_2\underline{C}H_3$), *δ* 24.16 ($\underline{C}H_2CH(PO(O\underline{CH_3}CH_2)_2)_2$), *δ* 34.29 (t, ^{1}Jcp = 214.1, $CH_2\underline{C}H(PO(O\underline{CH_3}CH_2)_2)_2$), *δ* 46.34 ($CH_2NH\underline{C}H_2$), *δ* 47.79 ($Cp\underline{C}H_2NHCH_2$), *δ* 62.8 (q, ^{2}Jcp = 10.1, $O\underline{C}H_2CH_3$), *δ* 68.42 (CH-subst. Cp), *δ* 68.58 (Cp unsubst.), *δ* 69.25 (CH-subst. Cp). HRMS (ESI^+): calcd *m/z*: 530.1524 $[M+H]^+$; found: 530.1531 $[M+H]^+$

4.5. Cell lines and cell culture

The human cancer cell lines, A549 and HeLa, as well as normal murine fibroblast cells (NIH3T3) were purchased from Cellonex, Separations (Randburg, South Africa) A549 and HeLa cells were cultured in Dulbecco's Modified Eagle's Medium (DMEM); while NIH3T3 was grown in Roswell Park Memorial Institute medium 1640 (RPMI 1640). Both culture media were supplemented with 10% heat-inactivated foetal bovine serum, 2 mM L-glutamine, 100 μg/mL streptomycin and 100 Units/mL penicillin and incubated at 37 °C in a humified atmosphere containing 5% of CO_2.

4.6. Cytotoxicity assay

The antiproliferative activity of the synthesized hybrids was evaluated using an Alamar Blue (7-hydroxy-10-oxidophenoxazin-10-ium-3-one) cell viability assay which quantitatively measures cell viability and proliferation. The Alamar Blue (resazurin) dye contains an oxidation–reduction indicator that both fluoresces and changes colour in response to the chemical reduction of the growth medium due to cell growth.

Exponentially growing cells (A549, HeLa and NIH3T3) were seeded in 96-well plates (20,000 cells/ml in a well plate) and, after 24 h of growth, were treated with increasing concentrations (6.25, 12.5, 25, 50 and 100 μg/ml) of the tested compounds, paclitaxel and cisplatin. These compounds were dissolved in 0.1% DMSO and 99.9% phosphate-buffered saline (PBS). Negative control cells were treated with 0.1% of DMSO. After 48 h of incubation, 10 μL of Alamar Blue was added to each well plate and incubated once again at 37 °C for 4 h. The cell viability/inhibition was estimated by measuring the absorbance at 570 nm and 600 nm (for background correction) in a microplate reader (VICTOR X3 2030 Multi-Label Plate Reader, Perkin Elmer, MA, USA). Calculation of IC_{50} was done using GraphPad Prism software (GraphPad, CA, USA)

4.7. Insilico molecular docking

4.7.1. Protein preparation

Molecular docking was performed using the Maestro (Schrodinger Release 2000-3). The X-ray crystallography structure of representative drug targets in the A549 cell and HeLa cell lines were retrieved from PDB (http://www.pdb.org). To ensure the structural correctness of these crystal structures, they were processed using the protein preparation wizard panel available on the Schrodinger suite. The molecules were hydrogenated, and bond orders were assigned while water molecules and other heteroatoms were deleted. Finally, optimization and energy minimization was performed by applying the default constraint of 0.3 Å RMSD (root-mean-square-deviation) and OPLS3e force field. The OPLS3e force field was used to optimize the proteins because it is having the advantage of predicting protein − ligand binding affinities to high accuracy.[65,66]

4.7.2. Ligand preparation

F1 and **H6** were used in the docking process because of their high cytotoxicity. Structural optimization was achieved with the help of the LigPrep panel on the Schrodinger suite. The possible protonation states were generated for each ligand using the Epik module at a pH of 7.0. One conformation for each of the ligands was generated, and all other parameters were kept default.

4.7.3. Grid generation and docking

Prior to docking analysis, the binding pocket of some of the proteins were searched in the literature while others were predicted with the help of the binding pocket prediction server, CastP.[67] The Ligand Docking with extra precision (XP) mode of the Glide module on the Schrodinger suite was used to dock the ligand to their corresponding protein. Finally, the binding free energy values, given in kcal/mol were obtained from the calculation. The higher negative binding free energy (BE) values indicate better ligand–protein interaction.[68]

Declaration of Competing Interest

The authors declare that they have no known competing financial interests or personal relationships that could have appeared to influence the work reported in this paper.

Acknowledgements

We acknowledge the financial assistance of the National Research

Foundation and Medical Research Council (Self-Initiated Research) South Africa. Samson.O. Oselusi thanks the Centre for High-Performance Computing (South Africa) for providing access to the computational resources used in this work.

Appendix A. Supplementary material

Supplementary data to this article can be found online at https://doi.org/10.1016/j.bmc.2022.116652.

References

1. Kerru N, Singh P, Koorbanally N, Raj R, Kumar V. Recent advances (2015–2016) in anticancer hybrids. *Eur J Med Chem*. 2017;142:179–212. https://doi.org/10.1016/j.ejmech.2017.07.033.
2. Boudhar A, Ng XW, Loh CY, et al. Overcoming chloroquine resistance in malaria: design, synthesis and structure-activity relationships of novel hybrid compounds. *Antimicrob Agents Chemother*. 2016;60(5):3076–3089. https://doi.org/10.1128/AAC.02476-15.
3. Xie SS, Wang XB, Li JY, Yang L, Kong LY. Design, synthesis and evaluation of novel tacrine-coumarin hybrids as multifunctional cholinesterase inhibitors against Alzheimer's disease. *Eur J Med Chem*. 2013;64. https://doi.org/10.1016/j.ejmech.2013.03.051.
4. Berube G. An overview of molecular hybrids in drug discovery. *Expert Opin Drug Discov*. 2016;0441(January):1–25. https://doi.org/10.1517/17460441.2016.1135125.
5. Xu Z, Zhang S, Gao C, et al. Isatin hybrids and their anti-tuberculosis activity. *Chinese Chem Lett*. 2017;28(2):159–167. https://doi.org/10.1016/j.cclet.2016.07.032.
6. Subhedar DD, Shaikh MH, Nawale L, et al. Novel tetrazoloquinoline–rhodanine conjugates: highly efficient synthesis and biological evaluation. *Bioorg Med Chem Lett*. 2016;26(9):2278–2283. https://doi.org/10.1016/j.bmcl.2016.03.045.
7. Zou Y, Yu S, Li R, et al. Synthesis, antifungal activities and molecular docking studies of novel 2-(2,4-difluorophenyl)-2-hydroxy-3-(1H–1,2,4-triazol-1-yl)propyl dithiocarbamates. *Eur J Med Chem*. 2014;74:366–374. https://doi.org/10.1016/j.ejmech.2014.01.009.
8. Gediya LK. Promise and challenges in drug discovery and development of hybrid anticancer drugs; 2009. p. 1099–111.
9. Wang R, Chen H, Yan W, Zheng M, Zhang T, Zhang Y. European Journal of Medicinal Chemistry Ferrocene-containing hybrids as potential anticancer agents : Current developments, mechanisms of action and structure-activity relationships. *Eur J Med Chem*. 2020;190:112109. https://doi.org/10.1016/j.ejmech.2020.112109.
10. Noh J, Kwon B, Han E, et al. Amplification of oxidative stress by a dual stimuli-responsive hybrid drug enhances cancer cell death. *Nat Commun*. 2015;6. https://doi.org/10.1038/ncomms7907.
11. Shou KJ, Li J, Jin Y, Lv YW. Design, synthesis, biological evaluation, and molecular docking studies of quinolone derivatives as potential antitumor topoisomerase I inhibitors. *Chem Pharm Bull*. 2013;61(6):631–636. https://doi.org/10.1248/cpb.c13-00040.
12. Duan Y, Xu S, Xiong H, et al. Discovery of novel 2-substituted-4-phenoxypyridine derivatives as potential antitumor agents. *Bioorganic Med Chem Lett*. 2018;28(3):254–259. https://doi.org/10.1016/j.bmcl.2017.12.063.
13. Hu Q, Yin L, Hartmann RW. Selective dual inhibitors of CYP19 and CYP11B2: Targeting cardiovascular diseases hiding in the shadow of breast cancer. *J Med Chem*. 2012;55(16):7080–7089. https://doi.org/10.1021/jm3004637.
14. Aggarwal S, Mahapatra MK, Kumar R, et al. Synthesis and biological evaluation of 3-tetrazolo steroidal analogs: Novel class of 5α-reductase inhibitors. *Bioorganic Med Chem*. 2016;24(4):779–788. https://doi.org/10.1016/j.bmc.2015.12.048.
15. Amin KM, Abou-Seri SM, Awadallah FM, Eissa AAM, Hassan GS, Abdulla MM. Synthesis and anticancer activity of some 8-substituted-7-methoxy-2H-chromen-2-one derivatives toward hepatocellular carcinoma HepG2 cells. *Eur J Med Chem*. 2015;90:221–231. https://doi.org/10.1016/j.ejmech.2014.11.027.
16. Liu MM, Chen XY, Huang YQ, et al. Hybrids of phenylsulfonylfuroxan and coumarin as potent antitumor agents. *J Med Chem*. 2014;57(22):9343–9356. https://doi.org/10.1021/jm500613m.
17. Wang Q, Guo Y, Jiang S, et al. A hybrid of coumarin and phenylsulfonylfuroxan induces caspase-dependent apoptosis and cytoprotective autophagy in lung adenocarcinoma cells. *Phytomedicine*. 2017;2018(39):160–167. https://doi.org/10.1016/j.phymed.2017.12.029.
18. Guo Y, Wang Y, Li H, et al. Novel nitric oxide donors of phenylsulfonylfuroxan and 3-benzyl coumarin derivatives as potent antitumor agents. *ACS Med Chem Lett*. 2018;9(5):502–506. https://doi.org/10.1021/acsmedchemlett.8b00125.
19. Gagnon V, St-Germain MÈ, Descôteaux C, et al. Biological evaluation of novel estrogen-platinum(II) hybrid molecules on uterine and ovarian cancers - molecular modeling studies. *Bioorganic Med Chem Lett*. 2004;14(23):5919–5924. https://doi.org/10.1016/j.bmcl.2004.09.015.
20. Smyre CL, Saluta G, Kute TE, Kucera GL, Bierbach U. Inhibition of DNA synthesis by a platinum-acridine hybrid agent leads to potent cell kill in nonsmall cell lung cancer. *ACS Med Chem Lett*. 2011;2(11):870–874. https://doi.org/10.1021/ml2001888.
21. Ouellette V, Côté MF, Gaudreault RC, Tajmir-Riahi HA, Bérubé G. Second-generation testosterone-platinum(II) hybrids for site-specific treatment of androgen receptor positive prostate cancer: design, synthesis and antiproliferative activity. *Eur J Med Chem*. 2019;179:660–666. https://doi.org/10.1016/j.ejmech.2019.06.090.
22. Mueller K, Schütz C, Rüffer T, et al. Synthesis, characterization, structures and in vitro antitumor activity of platinum(II) complexes bearing adeninato or methylated adeninato ligands. *Inorganica Chim Acta*. 2020;507(October 2019). https://doi.org/10.1016/j.ica.2020.119539.
23. Gupta A, Saha P, Descôteaux C, Leblanc V, Asselin É, Bérubé G. Design, synthesis and biological evaluation of estradiol-chlorambucil hybrids as anticancer agents. *Bioorganic Med Chem Lett*. 2010;20(5):1614–1618. https://doi.org/10.1016/j.bmcl.2010.01.053.
24. Osella D, Ferrali M, Zanello P, et al. On the mechanism of the antitumor activity of ferrocenium derivatives. *Inorganica Chim Acta*. 2000;306(1):42–48. https://doi.org/10.1016/S0020-1693(00)00147-X.
25. El Arbi M, Pigeon P, Top S, et al. Evaluation of bactericidal and fungicidal activity of ferrocenyl or phenyl derivatives in the diphenyl butene series. *J Organomet Chem*. 2011;696(5):1038–1048. https://doi.org/10.1016/j.jorganchem.2010.09.015.
26. Plazuk D, Vessières A, Hillard EA, et al. A [3]ferrocenophane polyphenol showing a remarkable antiproliferative activity on breast and prostate cancer cell lines. *J Med Chem*. 2009;52(15):4964–4967. https://doi.org/10.1021/jm900297x.
27. Spoerlein-Guettler C, Mahal K, Schobert R, Biersack B. Ferrocene and (arene) ruthenium(II) complexes of the natural anticancer naphthoquinone plumbagin with enhanced efficacy against resistant cancer cells and a genuine mode of action. *J Inorg Biochem*. 2014;138:64–72. https://doi.org/10.1016/j.jinorgbio.2014.04.020.
28. Jia DG, Zheng JA, Fan YR, et al. Ferrocene appended naphthalimide derivatives: synthesis, DNA binding, and in vitro cytotoxic activity. *J Organomet Chem*. 2019;888:16–23. https://doi.org/10.1016/j.jorganchem.2019.03.001.
29. Milutinović MM, Čanović PP, Stevanović D, et al. Newly synthesized heteronuclear ruthenium(II)/ferrocene complexes suppress the growth of mammary carcinoma in 4T1-treated BALB/c mice by promoting activation of antitumor immunity. *Organometallics*. 2018;37(22):4250–4266. https://doi.org/10.1021/acs.organomet.8b00604.
30. Narváez-Pita X, Rheingold AL, Meléndez E. Ferrocene-steroid conjugates: synthesis, structure and biological activity. *J Organomet Chem*. 2017;846(August):113–120. https://doi.org/10.1016/j.jorganchem.2017.06.004.
31. Esparza-Ruiz A, Herrmann C, Chen J, Patrick BO, Polishchuk E, Orvig C. Synthesis and in vitro anticancer activity of ferrocenyl-aminoquinoline- carboxamide conjugates. *Inorganica Chim Acta*. 2012;393:276–283. https://doi.org/10.1016/j.ica.2012.06.039.
32. Guo Y, Wang SQ, Ding ZQ, Zhou J, Ruan BF. Synthesis, characterization and antitumor activity of novel ferrocene bisamide derivatives containing pyrimidine-moiety. *J Organomet Chem*. 2017;851:150–159. https://doi.org/10.1016/j.jorganchem.2017.09.032.
33. Quirante J, Dubar F, González A, et al. Ferrocene-indole hybrids for cancer and malaria therapy. *J Organomet Chem*. 2011;696(5):1011–1017. https://doi.org/10.1016/j.jorganchem.2010.11.021.
34. Kowalski K, Hikisz P, Szczupak Ł, Therrien B, Koceva-Chyła A. Ferrocenyl and dicobalt hexacarbonyl chromones - new organometallics inducing oxidative stress and arresting human cancer cells in G2/M phase. *Eur J Med Chem*. 2014;81:289–300. https://doi.org/10.1016/j.ejmech.2014.05.023.
35. Pérès B, Nasr R, Zarioh M, et al. Ferrocene-embedded flavonoids targeting the Achilles heel of multidrug-resistant cancer cells through collateral sensitivity. *Eur J Med Chem*. 2017;130(December):346–353. https://doi.org/10.1016/j.ejmech.2017.02.064.
36. Maschke M, Lieb M, Metzler-Nolte N. Biologically active trifluoromethyl-substituted metallocene triazoles: characterization, electrochemistry, lipophilicity, and cytotoxicity. *Eur J Inorg Chem*. 2012;36:5953–5959. https://doi.org/10.1002/ejic.201200798.
37. Hafez TS, Osman SA, Yosef HAA, et al. Synthesis, structural elucidation, and in vitro antitumor activities of some pyrazolopyrimidines and schiff bases derived from 5-amino-3-(arylamino)-1H-pyrazole-4-carboxamides. *Sci Pharm*. 2013;81(2):339–357. https://doi.org/10.3797/scipharm.1211-07.
38. Bansode P, Patil P, Choudhari P, et al. Anticancer activity and molecular docking studies of ferrocene tethered ionic liquids. *J Mol Liq*. 2019;290:111182. https://doi.org/10.1016/j.molliq.2019.111182.
39. Gnant M, Clézardin P. Direct and indirect anticancer activity of bisphosphonates: a brief review of published literature. *Cancer Treat Rev*. 2012;38(5):407–415. https://doi.org/10.1016/j.ctrv.2011.09.003.
40. Sun Y, Chen L, Wu X, Ding Q. Bifunctional bisphosphonate derivatives and platinum complexes with high affinity for bone hydroxyapatite. *Bioorganic Med Chem Lett*. 2017;27(4):1070–1075. https://doi.org/10.1016/j.bmcl.2016.12.050.
41. Agyin JK, Santhamma B, Roy SS. Design, synthesis, and biological evaluation of bone-targeted proteasome inhibitors for multiple myeloma. *Bioorganic Med Chem Lett*. 2013;23(23):6455–6458. https://doi.org/10.1016/j.bmcl.2013.09.043.
42. Abdou WM, Barghash RF, Sediek AA. Design of new arylamino-2-ethane-1,1-diyl- and benzoxazole-2-methylene- bisphosphonates vs cytotoxicity and chronic inflammation diseases. from hydrophobicity prediction to synthesis and biological evaluation. *Eur J Med Chem*. 2012;57:362–372. https://doi.org/10.1016/j.ejmech.2012.09.032.
43. Reinholz MM, Zinnen SP, Dueck AC, et al. A promising approach for treatment of tumor-induced bone diseases: utilizing bisphosphonate derivatives of nucleoside antimetabolites. *Bone*. 2010;47(1):12–22. https://doi.org/10.1016/j.bone.2010.03.006.

44. Wang Z, Barrows RD, Emge TJ, Knapp S. Stereochemical Aspects of T3P Amidations. *Org Process Res Dev*. 2017;21(3):399–407. https://doi.org/10.1021/acs.oprd.7b00046.
45. Montalbetti CAGN, Falque V, Park M, Ox A. Amide bond formation and peptide coupling. *Tetrahedron*. 2005;61(740):10827–10852. https://doi.org/10.1016/j.tet.2005.08.031.
46. Allyn M, Kaufmann JPK. Lysosomal sequestration of amine-containing drugs: analysis and therapeutic implications. *J Pharm Sci*. 2007;96(4):729–746.
47. Mukaya HE, Mbianda XY. Macromolecular co-conjugate of ferrocene and bisphosphonate: synthesis, characterization and kinetic drug release study. *J Inorg Organomet Polym Mater*. 2015;25(3):411–418. https://doi.org/10.1007/s10904-015-0205-6.
48. Cai Y, Gao Y, Luo Q, et al. Ferrocene-grafted photochromic triads based on a sterically hindered ethene bridge: redox-switchable fluorescence and gated photochromism. *Adv Opt Mater*. 2016;4(9):1410–1416. https://doi.org/10.1002/adom.201600229.
49. Kieczykowski GR, Jobson RB, Melillo DG, Reinhold DF, Grenda VJ, Shinkai I. Preparation of (4-Amino-1-Hydroxybutylidene)bisphosphonic acid sodium salt, MK-217 (Alendronate Sodium). An improved Procedure for the Preparation of 1-Hydroxy-1,1-bisphosphonic Acids. *J Org Chem*. 1995;60(25):8310–8312. https://doi.org/10.1021/jo00130a036.
50. Ferrer-Casal M, Barboza AP, Szajnman SH, Rodriguez JB. 1,3-dipolar cycloadditions of the versatile intermediate tetraethyl vinylidenebisphosphonate. *Synth*. 2013;45(17):2397–2404. https://doi.org/10.1055/s-0033-1338498.
51. Simoni D, Gebbia N, Invidiata FP, et al. Design, synthesis, and biological evaluation of novel aminobisphosphonates possessing an in vivo antitumor activity through a γδ -T lymphocytes-mediated activation mechanism. *J MedChem*. 2008;51:6800–6807.
52. Hochdörffer K, Abu Ajaj K, Schäfer-Obodozie C, Kratz F. Development of novel bisphosphonate prodrugs of doxorubicin for targeting bone metastases that are cleaved pH dependently or by cathepsin B: synthesis, cleavage properties, and binding properties to hydroxyapatite as well as bone matrix. *J Med Chem*. 2012;55(17):7502–7515. https://doi.org/10.1021/jm300493m.
53. Hu JR, Zhang WJ, Huang HJ, Wang YH. Synthesis of N-ferrocenylmethyleneglycine. *Huaxue shijie*. 2012;34(10):949–951.
54. Aderibigbe BA, Varaprasad K, Sadiku ER, et al. Kinetic release studies of nitrogen-containing bisphosphonate from gum acacia crosslinked hydrogels. *Int J Biol Macromol*. 2015;73(1):115–123. https://doi.org/10.1016/j.ijbiomac.2014.10.064.
55. Alver Ö, Parlak C. FT-IR, NMR spectroscopic and quantum mechanical investigations of two ferrocene derivatives. *Bull Chem Soc Ethiop*. 2017;31(1):63–74.
56. Corry AJ, Goel A, Alley SR, et al. N-ortho-Ferrocenyl benzoyl dipeptide esters: synthesis, structural characterization and in vitro anti-cancer activity of N-{ortho-(ferrocenyl)benzoyl}-glycine-l-alanine ethyl ester and N-{ortho-(ferrocenyl) benzoyl}-l-alanine-glycine ethyl ester. *J Organomet Chem*. 2007;692(6 SPEC. ISS.):1405–1410. https://doi.org/10.1016/j.jorganchem.2006.10.018.
57. Babin VN, Belousov YA, Borisov VI, et al. Ferrocenes as potential anticancer drugs. *Russ Chem Bull Int Version*. 2014;63(11):2405–2422. https://0-link.springer.com.wagtail.ufs.ac.za/content/pdf/10.1007%2Fs11172-014-0756-7.pdf.
58. Sathyadevi P, Krishnamoorthy P, Butorac RR, Cowley AH, Dharmaraj N. Synthesis of novel heterobimetallic copper(i) hydrazone Schiff base complexes: a comparative study on the effect of heterocyclic hydrazides towards interaction with DNA/protein, free radical scavenging and cytotoxicity. *Metallomics*. 2012;4(5):498–511. https://doi.org/10.1039/c2mt00004k.
59. Adeyemo A, Shettar A, Bhat IA, Kondaiah P, Mukherjee PS. Self-assembly of discrete ruii8 molecular cages and their in vitro anticancer activity. *Inorg Chem*. 2017;56(1):608–617. https://doi.org/10.1021/acs.inorgchem.6b02488.
60. Qin QP, Zou BQ, Tan MX, et al. High in vitro anticancer activity of a dinuclear palladium(II) complex with a 2-phenylpyridine ligand. *Inorg Chem Commun*. 2018;96(June):106–110. https://doi.org/10.1016/j.inoche.2018.08.007.
61. Wang F, Li Y, Zhang Z, Wang J, Wang J. SHCBP1 regulates apoptosis in lung cancer cells through phosphatase and tensin homolog. *Oncol Lett*. 2019;18(2):1888–1894. https://doi.org/10.3892/ol.2019.10520.
62. Borappa K, Sivakumari K. In silico docking of quercetin compound aginst the HeLa cell line proteins. *Intl J Curr Pharm Res*. 2019;7(1):13–16.
63. Oyewusi HA, Huyop F, Wahab RA. Molecular docking and molecular dynamics simulation of Bacillus thuringiensis dehalogenase against haloacids, haloacetates and chlorpyrifos. *J Biomol Struct Dyn*. 2020:1–16. https://doi.org/10.1080/07391102.2020.1835727.
64. Hardouin J, Guénin E, Monteil M, Caron M, Lecouvey M. Fragmentation patterns of new esterified and unesterified aromatic 1-hydroxymethylene-1,1-bisphosphonic acids by ESI-MSn. *J Mass Spectrom*. 2008;43(8):1037–1044. https://doi.org/10.1002/jms.1379.
65. Desai N, Mahto MK, Alekhya B, Naveen CR, Bhaskar M. Comparative docking studies of Estrogen Receptor inhibitors and their binding interaction analysis. *Int J Pharm Sci Rev Res*. 2012;16(1):91–95.
66. Harder E, Damm W, Maple J, et al. OPLS3: a force field providing broad coverage of drug-like small molecules and proteins. *J Chem Theory Comput*. 2016;12(1):281–296. https://doi.org/10.1021/acs.jctc.5b00864.
67. Binkowski TA, Naghibzadeh S, Liang J. CASTp: computed atlas of surface topography of proteins. *Nucleic Acids Res*. 2003;31(13):3352–3355. https://doi.org/10.1093/nar/gkg512.
68. Dallakyan S, Olson AJ. Small-molecule library screening by docking with PyRx. *Methods Mol Biol*. 2015;1263(January):243–250. https://doi.org/10.1007/978-1-4939-2269-7_19.